VIJAY KUMAR GARG [1,2,*], **SUDHIR SHARMA** [3]

Regular paper

Hardware implementation of wind turbine emulator and its integration with utility grid

Worldwide, renewable energy sources, mainly wind and solar power, prove their efficacy to provide a sustainable solution to meet the growing energy demand. Research and investigation on a natural system are uneconomical and depend upon various environmental and seasonal circumstances. The wind emulator can replicate the static and dynamic behavior of a realistic wind turbine system. This paper presents the wind energy conversion system (WECS) using the wind turbine emulator (WTE) hardware model. The mathematical model of wind turbine has been developed using LabVIEW. The WTE consists DC shunt motor coupled with a three-phase self-excited induction generator (SEIG), which is further integrated with the utility grid through a DC microgrid. Various types of control devices such as DC-DC converter, current PI controller, speed PI controller, rectifier, etc., are employed to control the emulator's performance concerning the rotational speed of the wind turbine. The NI-sbRIO-9607 data card and the graphical user interface (GUI) based on the LabVIEW system provide real-time data acquisition and flexibility in the variation of wind speed and various turbine parameters during experimental validation of WECS. The energy flow with the utility grid, static and dynamic characteristics under different wind speeds are successfully emulated by the experimental setup of a wind turbine emulator.

Keywords: Wind turbine emulator; wind energy conversion system; buck converter; DC microgrid; grid integration; hardware model.

1. Introduction

Worldwide, electricity usage is growing due to increasing prosperity and living standards with an annual increment of 1-2%, except the financial crisis in 1980 and 2009 [1]. The scientific and technological advancement in power generation from renewable energy sources makes them cost-competitive, further increasing their penetration rate. Wind power is one of the prominent and fastest-growing renewable energy sources. The cumulative installed capacity of wind energy in India is depicted in Figure 1.India has made tremendous efforts in the renewable energy field by establishing a ministry for renewables. Now, globally, India stands at 4th position in renewable energy installation capacity[2]. The detailed analysis of the wind energy conversion system (WECS), composed of various electrical and power electronics components, improves their efficiency and performance in a realistic environment.

Electricity production from wind energy depends upon various geographical and environmental factors. It is time-consuming and uneconomical to realize WECS in natural conditions. The schematic diagram of WECS is shown in Figure 2 [3]. A natural wind turbine system's static and dynamic behavior can be analyzed with Wind Turbine Emulator (WTE) without dependency on a natural source and wind turbine [4], [5]. In the laboratory, the investigation can be performed on the actual behavior of WECS, control strategies, and testing of new technologies. Various motors can be used in wind turbine emulators, such as

* Corresponding author: Vijay Kumar Garg, Assistant Professor, UIET, Kurukshetra University, Kurukshetra, India, E-mail: vkgarg.ee@gmail.com
[1] (Research Scholar) IKG Punjab Technical University, Jalandhar, India
[2] Department of Electrical Engineering, UIET, Kurukshetra University, Kurukshetra, India
[3] Department of Electrical Engineering, DAV Institute of Engineering and Technology, Jalandhar, India

permanent magnet synchronous motor (PMSM), squirrel cage induction motor, doubly fed induction motor, and DC motor-driven system [6].

In the literature, various studies have been performed using simulation/hardware environments. A hardware-based laboratory emulator helps in a realistic investigation of WECS without relying on natural sources [7]. A detailed analysis of wind emulators for static and dynamic performance evaluation has been presented in [8]. The authors proposed two coupled squirrel cage induction machines, DSP-enabled software system. An experimental investigation has been performed using PMSM, IGBT-based inverter, and PI-controlled based hardware system for various characteristics of WECS [9].Similarly, the dynamic performance of WECS has been validated using an FPGA-based wind turbine system consisting of a DC motor in the Xilinx System Generator (XSG) [3]. The validation of results has been performed under variations such as wind speed, load, and other conditions. Similar types of validation for various characteristics have been conducted through hardware models by multiple researchers [9]–[12]. Validation of the λ-CP curve for small windmills is costly and complex. The authors in [13] proposed λ-CP characteristics from a small wind turbine emulator in real operating conditions, improving the overall design process. Integration of renewable energy sources with the electricity grid affects the power quality of the distribution system. The authors in [14] investigated the various power quality issues with experimental setup for a wind energy system.
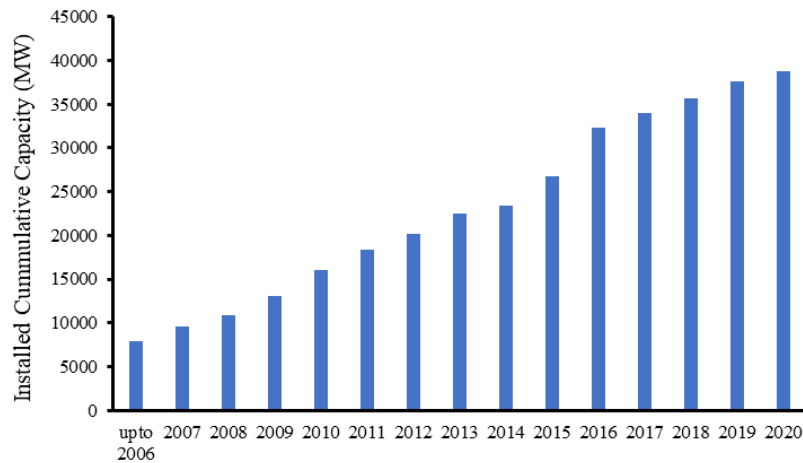

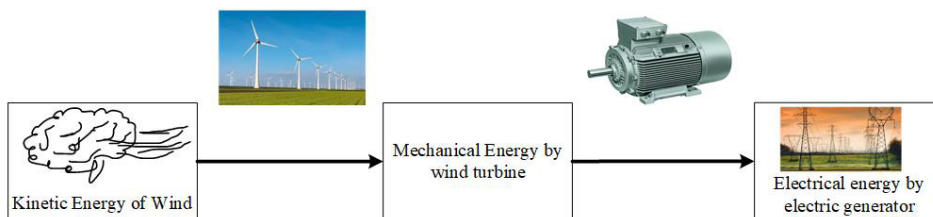Figure 1: Cumulative installed wind capacity of India

Figure 2: Schematic diagram of WECS

In this paper, DC-SEIG based wind turbine emulator is considered, and real-time analysis is performed using data acquisition through NI card with hardware model using the graphical user interface (GUI) based on LabVIEW. Section 2 presents the mathematical modeling of the wind turbine system. Section 3 describes the wind turbine emulator and the experimental setup of the hardware system. The performance of WTE and its various characteristics is presented and discussed in section 4. The conclusion and future scope are discussed in section 5.

2. Mathematical model of Wind Turbine system

The wind flow is erratic and unpredictable. The WTE can emulate the characteristics of the wind turbine system. The mechanical power capture by the wind turbine, P in kW, is given as[15]–[17]:

$$P_{WT} = \frac{1}{2} \rho \pi R^2 C_P(\lambda, \beta) V_W^3 \tag{1}$$

Where ρ represents the air density in kg/m^3; R asthe radius of a turbine blade in meter; C_P denotes power coefficient; λ denotes the tip speed ratio; β defines the blade pitch angle in degree and V_W wind speed in m/sec at hub height. Air density varies due to environmental factors like temperature, atmospheric pressure. The tip speed ratio can be expressed as[18]:

$$\lambda = \frac{\omega_T R}{V_W} \tag{2}$$

Where ω_T denotes the angular speed in rad/sec.
C_P can be expressed as [15], [19]:

$$C_P(\lambda, \beta) = c_1 \left(\frac{C_2}{\lambda_i} - c_3 \beta - c_4 \right) e^{\frac{-C_5}{\lambda_i}} + c_6 \lambda \tag{3}$$

$$\frac{1}{\lambda_i} = \frac{1}{\lambda + 0.08\beta} - \frac{0.035}{\beta^3 + 1} \tag{4}$$

The various values of C_P coefficients are presented in Table 1. The wind turbine torque can be expressed as:

$$T_{WT} = \frac{1}{2} \frac{\rho \pi R^3 C_P(\lambda, \beta) V_W^2}{\lambda} \tag{5}$$

Table 1: Coefficients for C_P calculation

C_1	C_2	C_3	C_4	C_5	C_6
0.5176	116	0.4	5	21	0.0068

The mechanical model of a real and hardware model of wind turbine system is depicted in Figure 3 [20], [21].

The equivalent circuit of DC motor is depicted in Figure 4. The mathematical equations for an ideal model neglecting armature reaction, and mechanical losses are as follow[22], [23]:

$$V_t = I_a R_a + L_a \frac{dI_a}{dt} + E_b \qquad (6)$$

$$E_b = K_a \phi \omega_m \qquad (7)$$

$$T_m = K_t \phi I_a \qquad (8)$$

$$T_M - T_G = J_M \frac{d\omega_G}{dt} + B\omega_M \qquad (9)$$

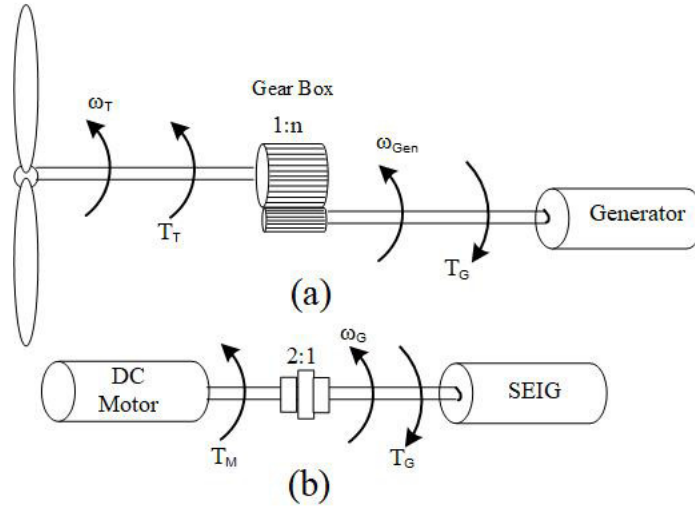where K_a and K_t are armature and torque constant.
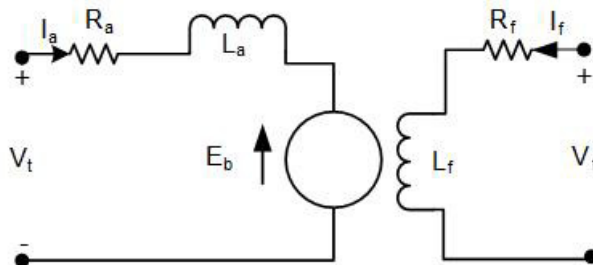

Figure3:Mechanical Model of (a) Real (b)WTE

Figure 4: Equivalent circuit of DC motor

3. Wind Turbine Emulator

Wind turbine emulators replicate the actual wind turbine behavior. The motor is derived as per actual wind turbine characteristics in the wind park. The mathematical model of the WT is developed in LabVIEW using various mathematical equations describing its features. A user interface GUI system has been designed for multiple inputs and real-time display of parameters. The various inputs of themodel of WT are pitch angle (β), wind

speed in m/s, andangular speed of the generator. Generator speed is sensed by tachogenerator, which is further converted into voltage signal after gear ratio conversion and fed in the form of speed signal in LabVIEW model through NI card. The control scheme of WTE is depicted in Figure 5. The wind turbine model provides the reference torque for the drive arrangement. After proper conditioning,a reference current is producedfrom reference torque and compared with the armature current of the DC motor.The error signal is fed into the Proportional-Integral (PI) controller, further processed through the pulse width modulation (PWM) control circuit. The gate pulses produced by the PWM circuitare amplified to a value, which can trigger the gate circuit of the buck converter's IGBT. DC/DC buck converter controls the armature voltage of the DC motor. The motor current and speed change, which further varies parameters, and the system reaches a steady state.
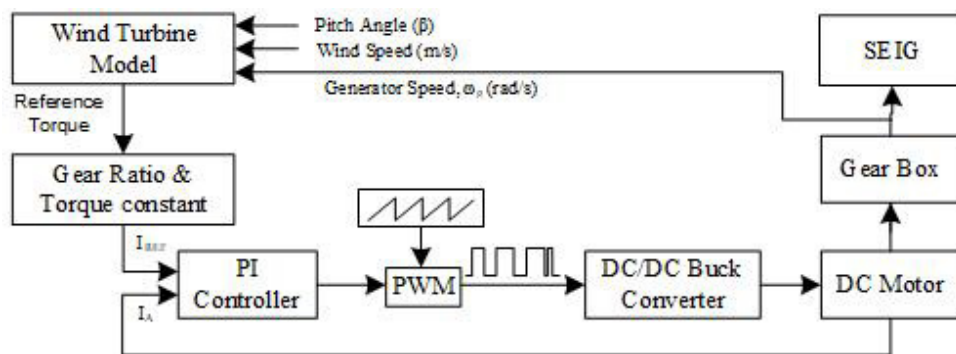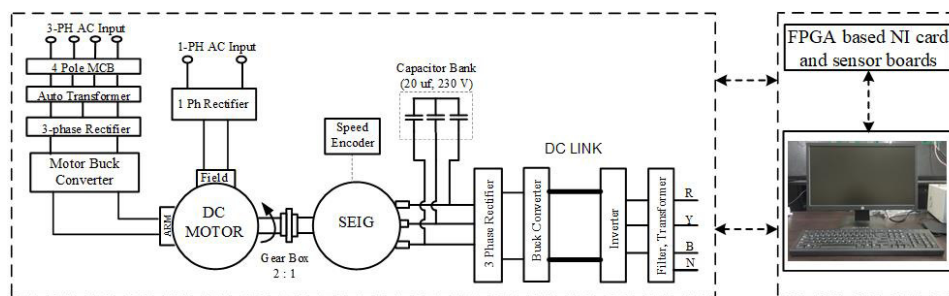

Figure 5:Control scheme of wind turbine emulator

Figure 6:Block diagram of the hardware model

The block diagram of the hardware model is depicted in Figure 6. The torque produced by the real wind energy is redeveloped with the help of a DC motor. The system consists 5 HP DC motor, which is controlled by DC drive. The field winding is supplied through a single-phase rectifier, whereas the armature winding is through a three-phase rectifier connected through a buck converter. DC motor is mechanical coupled to self-excited induction generator (SEIG) through gearbox having a gear ratio of 2:1 [24]. The alternating current produced by SEIG is fed to the rectifier and buck converter. The battery energy

storage system is connected to DC Bus through a bidirectional buck-boost converter. The DC Bus is connected to the grid through a three-phase rectifier, LC filter, and delta to star step-up transformer.
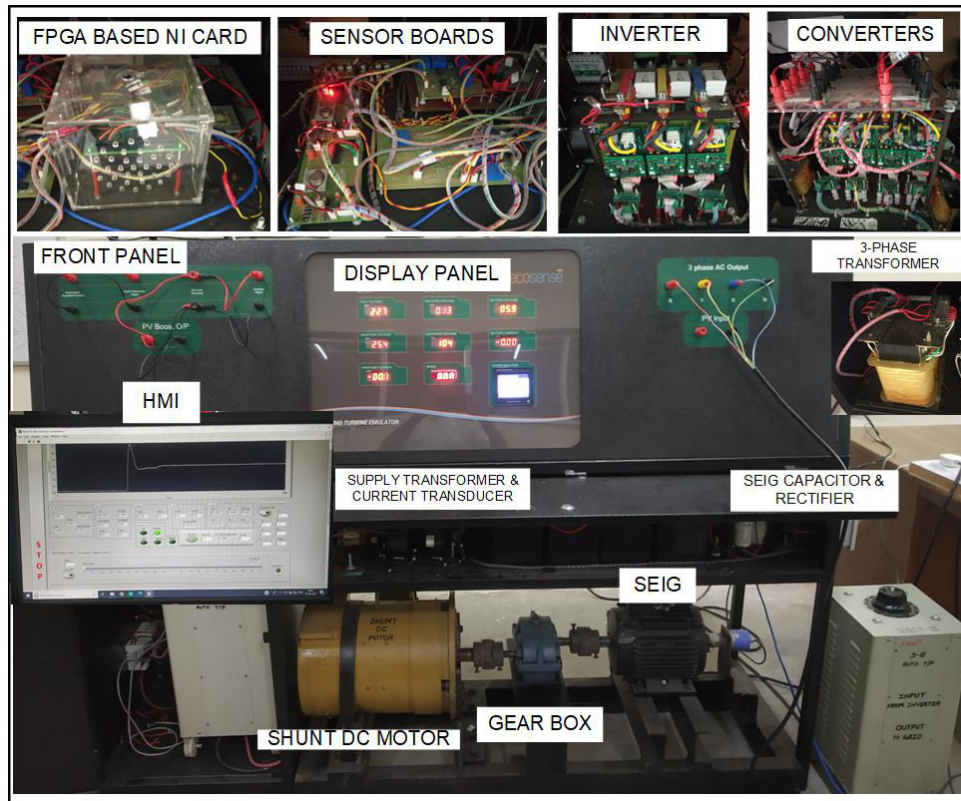

Figure 7:Experimental setup of grid integrated WTE

The experimental setup of grid integrated DC microgrid consisting of wind emulator is shown in Figure 7.The output of WTE is connected through a boost converter with a DC link, having a voltage range of 110-150V. Data acquisition has been performed through FPGA based NI-sbRIO-9607 (National Instruments) data card. It is connected to the primary system through CAT-5 or above LAN cable with RJ-45 gigabit ethernet port. The input and output operating signal range from 0-5V. All quantities are measured through various transducers and scaled in the operating range. The DC microgrid is connected with the utility grid through a three-phase autotransformer.

4. Result and discussion

To start the hardware model, the armature and field voltage of the DC motor is maintained as 250V and 220V, respectively, through a three-phase and single-phase autotransformer. The initial voltage of the DC link side is set at around 100 V through a three-phase autotransformer connected atthe grid side. The human-machine interface (HMI) system, a LabVIEW-enabled GUI system, synchronize the DC link voltage at 120V

336

through an inverter. The various inputs and outputs are managed through the GUI system. The wind profile is varied as per the requirement of the characteristics.

4.1. Static behavior of WTE

The static characteristics of the WTE are observed by running the system at a constant speed. The wind speed is varied from 5m/s to 7.8 m/s, and corresponding values of the torque and speed w.r.t. change in rotor speed is observed. The torque and power characteristics of the wind turbine emulator at different wind speed values are given in Figure 8 (a) and (b), respectively. As the wind speed increases, the torque and power produced by the wind turbine also increase.
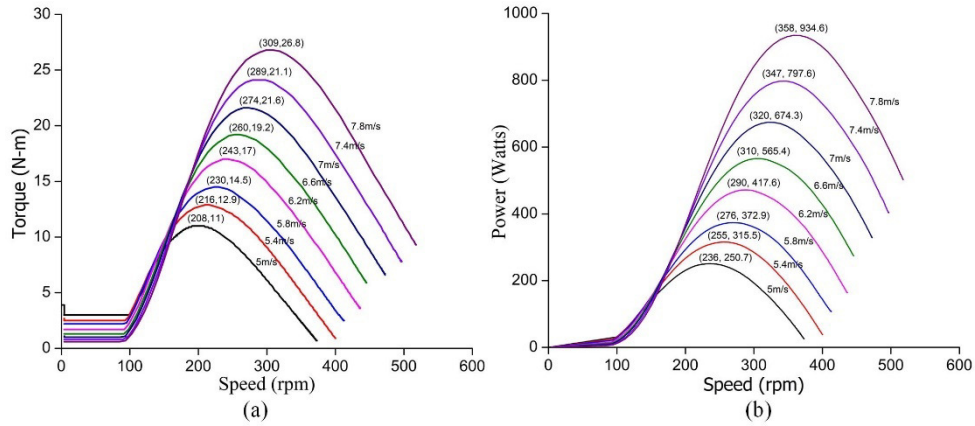

Figure 8: Variation of (a)Torque vs. Speed (b) Power vs. Speed for the various value of wind speed

The power coefficient, C_P represents the fraction of power extracted from wind energy. It varies with wind speed, turbine rotational speed, and turbine blade parameters. The variation of power coefficient, C_P with tip speed ratio, λ with change in blade pitch angle, β is represented in Figure9.
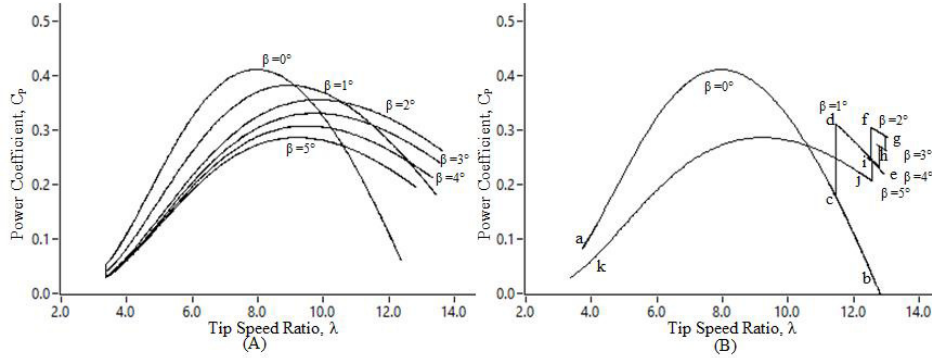

Figure 9: Variation of C_P-λ with different pitch angle, β

The Figure 9 represents the variation with blade pitch angle, β at a constant wind speed of 5 m/s.Part (A) of Figure9 shows the variation when angle β is varied while WTE is at the stop position. Therefore for each change in β, there is a separate curve. In part (B), the WTE continues to run, and angle β is increased by one factor. When $\beta=0°$, the curve follow the path ab, with change in angle to 1°, the curve moves to point c and further moves from point d to e. while a continuous increase of one degree in angle β from 2° to 5°, the pointer moves to f-g, h, i and j. When WTE is switched off,the curve finally comes to point k.Both of these characteristics resemble that with an increase in pitch angle, the maximum value of C_P reduces, which shows the reduction in extracted wind power.

4.2. Dynamic behavior of WTE

The dynamic behavior of WTE is experimentally validated with random variation in wind speed, and the variation of various factors is depicted in Figure 10. The speed of wind is varied as 5m/s, 6 m/s, 7 m/s, 6.5 m/s and 5.5 m/s as shown in Figure 10 (a). The experimental setup is run for a particular speed, and variation of different factors is noted.
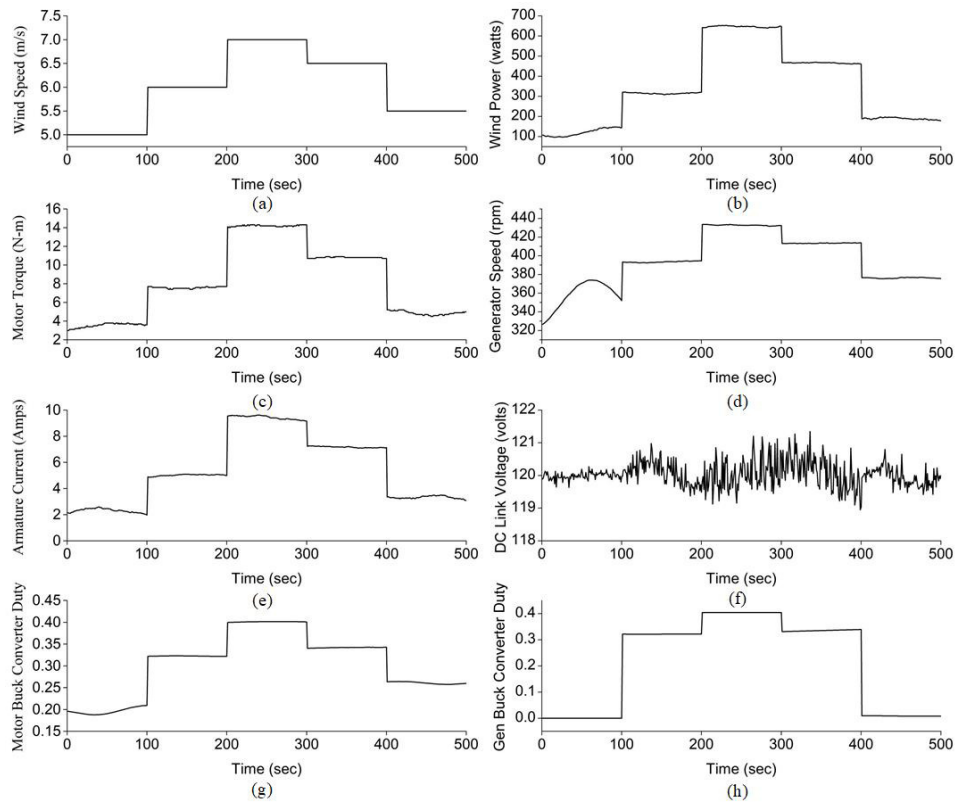
Figure 10: Dynamic response of different parameters with random variation in wind speed.

The motor's wind power and torque vary with wind speed variation, as shown in Figures 11(b) and (c). The generator speed fluctuates at a wind speed of 5 m/s, and after that, they vary as wind speed varies. The variation in armature current and DC link voltage is drawn in Figures 10 (e) and (f), respectively. The armature current rises with an increase in wind speed. The deviation in DC link voltage is minimum; however, it increases slightly with a rise in power generation due to increased wind speed. The duty of the motor side buck converter varies from 0.195 to 0.415, whereas the generator side buck converter varies from 0 to 0.417. The wide variation of buck and boost converter duty is shown in Figures 10 (g) and (f), respectively.

The hardware system of WTE is connected with the utility grid through a DC microgrid. The electricity requirement of the hardware and energy produced by WTE can be feed into the electricity grid. The input voltage of DC motor field winding, armature winding, and DC link voltage are 220V, 250V, and 120V. The filed voltage and DC link voltage remain approximately the same throughout the experiment. The variation of various factors is evaluated with continuous rise in wind speed, and the results are presented in Table 2.

Table 2: Variation of various parameters with an increase in wind speed

S. N.	Wind Speed (m/s)	Armature Voltage (volts)	Armature Current(ams)	Rectified voltage (volts)	Speed (rpm)	Motor torque (N-m)	Motor power (watts)	Cp	λ	Power Generated (watts)	Grid Power	% THD	
												THD$_i$ (current)	THD$_v$ (voltage)
1	5	239	2.5	193	330-380	3.0-4.0	120-140	0.2	11.70	6	-16	1.7	316
2	5.2	237	2.8	206	370	4	150	0.15	11.62	7	-14	1.68	300
3	5.3	236	3.1	232	372	4.1	152	0.16	11.60	7	-13	1.66	285
4	5.5	235	3.5	260	380	4.2	165	0.16	11.58	8	-11	1.64	270
5	5.6	235	4.0	270	385	5.0	200	0.18	11.40	9	-10	1.62	265
6	5.8	234	4.2	280	398	5.8	230	0.18	11.31	11	-6	1.61	259
7	6.0	231	4.8	285	406	6.6	280	0.20	11.21	60	22	1.60	81.0
8	6.2	230	6.1	290	409	8.5	360	0.24	10.90	150	81	1.58	39.36
9	6.4	229	7.0	299	415	10.0	426	0.25	10.75	190	121	1.63	28.36
10	6.6	228	8.2	306	423	11.4	500	0.27	10.60	250	170	1.63	21.22
11	6.8	225	9.2	314	430	12.7	270	0.28	10.50	300	212	1.73	17.94
12	7.0	224	10.1	317	440	14.0	635	0.29	10.40	390	251	1.71	13.88
13	7.2	223	11	319	447	15.4	710	0.295	10.30	400	308	1.6	12.32
14	7.4	222	12	324	458	16.5	780	0.3	10.25	480	341	1.59	11.14
15	7.6	221	13.0	330	466	17.8	860	0.3	10.17	500	393	1.62	10.34
16	7.8	220	13.8	333	476	19.0	940	0.31	10.16	510	438	1.58	9.16
17	8.0	219	14.9	341	485	20.0	1034	0.32	10.11	600	487	1.62	8.33

Note: Negative sign shows power to import, and the positive sign represents the energy export to the utility grid

With the increase in wind speed, the armature voltage decreases, whereas the armature current and rectified voltage increase. As speed increase, the torque and motor power increase, value of C$_P$ increase, while λ reduces. The wind speed is varied continuously through GUI. As the wind increases, the power and torque produced by the WTE system increase. In starting, there is sluggish behavior of the system due to inertia, and as the wind speed increase, the system starts moving smoothly, and there is a slight even rise in power and torque. The experimental real-time curves of power with wind speed, power with generator speed, and torque with generator speed are presented in Figures 11 (a), (b), and (c), respectively.

At a wind speed of 3.5m/s, the system emulator starts running. At 5 m/s, the speed varies between 330-380 rpm. There is continuous variation in power and torque, which is also depicted in a circular motion in Figures 11 (b) and (c), respectively. Motor buck converter starts at a wind speed of 5.3m/s and generator speed of 372 rpm. With a further rise in wind speed, the curves become smooth. The power generated by the system increase so as the power transfer to the electricity grid increases. The system consumes power up to wind speed of 5.8 m/s and after that starts exporting the electricity to the utility grid. The inverter maintains the DC link voltage and frequency near 120V and 50 Hz. The THD % of voltage

remains near 1.6-1.7 %, whereas for current, it is higher at starting and reduces as the wind speed increase.
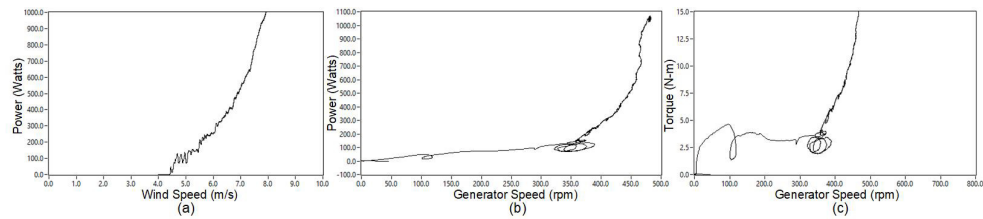

Figure 11: Experimental response of WTE with increase in wind speed (a) Power vs. Wind speed (b) Power vs. Generator speed (c) Torque vs. Generator speed

5. Conclusion

The unpredictable nature of the wind is the main obstacle tothe analysis of wind turbines in a natural system. In this paper, 5 HP DC motor drives the self-excited induction generator of 1 kW. The mechanical coupled motor-generator system with various control drives and converters resembles a real wind turbine system. The developed wind turbine emulator is controlled through LabVIEW enabled GUI system, real-time controllers, and data acquisition is performed through an NI card. The various static and dynamic behavior of the WTE has been achieved with the hardware system. The energy input, output, variation of current, power, torque, etc., have been analyzed with variation in wind speed. The effectiveness of the WTE is verified experimentally and in the future aim is to improve its effectiveness with demand-side management under different load conditions and wind variations.

Conflict of interests

The authors declare that they have no conflict of interest.

References

[1] BP, "BP Statistical Review of World Energy," 2020. Accessed: Dec. 15, 2020. [Online]. Available: https://www.bp.com/.

[2] S. Sharma and S. Sinha, "Indian wind energy & its development-policies-barriers: An overview," *Environ. Sustain. Indic.*, vol. 1–2, no. May, p. 100003, 2019, doi: 10.1016/j.indic.2019.100003.

[3] I. Moussa and A. Khedher, "A Theoretical and Experimental Study of a Laboratory Wind Turbine Emulator using DC-Motor Controlled by an FPGA-Based Approach," *Electr. Power Components Syst.*, vol. 48, no. 4–5, pp. 399–409, 2020, doi: 10.1080/15325008.2020.1793834.

[4] D. Thakur and J. Jiang, "Design and Construction of a Wind Turbine Simulator for Integration to a Microgrid with Renewable Energy Sources," *Electr. Power Components Syst.*, vol. 45, no. 9, pp. 949–963, 2017, doi: 10.1080/15325008.2017.1311385.

[5] P. K. Behera, B. Mendi, S. K. Sarangi, and M. Pattnaik, "Robust wind turbine emulator design using sliding mode controller," *Renew. Energy Focus*, vol. 36, no. March, pp. 79–88, 2021, doi: 10.1016/j.ref.2020.12.004.

[6] I. Moussa, A. Bouallegue, and A. Khedher, "New wind turbine emulator based on DC machine: Hardware

implementation using FPGA board for an open-loop operation," *IET Circuits, Devices Syst.*, vol. 13, no. 6, pp. 896–902, 2019, doi: 10.1049/iet-cds.2018.5530.

[7] J. R. De Oliveira and A. L. Andreoli, "Wind Turbine Emulator: A Tool for Experimental and Computational Study," *IEEE Lat. Am. Trans.*, vol. 19, no. 11, pp. 1832–1839, 2021, doi: 10.1109/tla.2021.9475616.

[8] J. Castelló, J. M. Espí, and R. García-Gil, "Development details and performance assessment of a Wind Turbine Emulator," *Renew. Energy*, vol. 86, pp. 848–857, 2016, doi: 10.1016/j.renene.2015.09.010.

[9] M. E. Abdallah, O. M. Arafa, A. Shaltot, and G. A. A. Aziz, "Wind turbine emulation using permanent magnet synchronous motor," *J. Electr. Syst. Inf. Technol.*, vol. 5, no. 2, pp. 121–134, 2018, doi: 10.1016/j.jesit.2018.03.005.

[10] P. Y. Chen, K. W. Hu, Y. G. Lin, and C. M. Liaw, "Development of a Prime Mover Emulator Using a Permanent-Magnet Synchronous Motor Drive," *IEEE Trans. Power Electron.*, vol. 33, no. 7, pp. 6114–6125, 2018, doi: 10.1109/TPEL.2017.2747221.

[11] L. K. Gan and E. J. P. Echenique Subiabre, "A realistic laboratory development of an isolated wind-battery system," *Renew. Energy*, vol. 136, pp. 645–656, 2019, doi: 10.1016/j.renene.2019.01.024.

[12] J. Yan, Y. Feng, and J. Dong, "Study on dynamic characteristic of wind turbine emulator based on PMSM," *Renew. Energy*, vol. 97, pp. 731–736, 2016, doi: 10.1016/j.renene.2016.06.034.

[13] C. I. Martínez-Márquez, J. D. Twizere-Bakunda, D. Lundback-Mompó, S. Orts-Grau, F. J. Gimeno-Sales, and S. Seguí-Chilet, "Small wind turbine emulator based on lambda-Cp curves obtained under real operating conditions," *Energies*, vol. 12, no. 13, 2019, doi: 10.3390/en12132456.

[14] O. P. Mahela, B. Khan, H. H. Alhelou, and S. Tanwar, "Assessment of power quality in the utility grid integrated with wind energy generation," *IET Power Electron.*, vol. 13, no. 13, pp. 2917–2925, 2020, doi: 10.1049/iet-pel.2019.1351.

[15] S. Heier, *Grid Integration of Wind Energy Conversion Systems*. John Wiley & Sons Ltd, 1998.

[16] A. Sajadi, Ł. Rosłaniec, M. Kłos, P. Biczel, and K. A. Loparo, "An emulator for fixed pitch wind turbine studies," *Renew. Energy*, vol. 87, no. September 2013, pp. 391–402, 2016, doi: 10.1016/j.renene.2015.10.033.

[17] M. A. Bhayo, M. J. A. Aziz, N. R. N. Idris, and A. H. M. Yatim, "Design and development of a wind turbine emulator for analyzing the performance of stand-alone wind energy conversion system," *Int. J. Power Electron. Drive Syst.*, vol. 8, no. 1, pp. 454–461, 2017, doi: 10.11591/ijpeds.v8i1.pp454-461.

[18] F. Martinez, L. C. Herrero, and S. de Pablo, "Open loop wind turbine emulator," *Renew. Energy*, vol. 63, pp. 212–221, 2014, doi: 10.1016/j.renene.2013.09.019.

[19] J. Hu, Y. Shan, Y. Xu, and J. M. Guerrero, "A coordinated control of hybrid ac/dc microgrids with PV-wind-battery under variable generation and load conditions," *Int. J. Electr. Power Energy Syst.*, vol. 104, no. April 2018, pp. 583–592, 2019, doi: 10.1016/j.ijepes.2018.07.037.

[20] J. Chen, J. Chen, C. Gong, and H. Wang, "Design and analysis of dynamic wind turbine simulator for wind energy conversion system," *IECON Proc. (Industrial Electron. Conf.*, pp. 971–977, 2012.

[21] M. Monfared, H. Madadi Kojabadi, and H. Rastegar, "Static and dynamic wind turbine simulator using a converter controlled dc motor," *Renew. Energy*, vol. 33, no. 5, pp. 906–913, 2008.

[22] N. C. Sahoo, A. S. Satpathy, N. K. Kishore, and B. Venkatesh, "D.c. motor-based wind turbine emulator using LabVIEW for wind energy conversion system laboratory setup," *Int. J. Electr. Eng. Educ.*, vol. 50, no. 2, pp. 111–126, 2013, doi: 10.7227/IJEEE.50.2.1.

[23] Himani and R. Dahiya, "Condition monitoring of a wind turbine generator using a standalone wind turbine emulator," *Front. Energy*, vol. 10, no. 3, pp. 286–297, 2016, doi: 10.1007/s11708-016-0419-5.

[24] P. Satish Kumar, R. P. S. Chandrasena, and K. Victor Sam Moses Babu, "Design and implementation of wind turbine emulator using FPGA for stand-alone applications," *Int. J. Ambient Energy*, vol. 0, no. 0, pp. 1–27, 2020, doi: 10.1080/01430750.2020.1736152.